

High-Order Multiple-Scattering Calculations of X-Ray-Absorption Fine Structure

J. J. Rehr,⁽¹⁾ R. C. Albers,⁽²⁾ and S. I. Zabinsky⁽¹⁾

⁽¹⁾*Department of Physics, University of Washington, Seattle, Washington 98195*

⁽²⁾*Theoretical Division, Los Alamos National Laboratory, Los Alamos, New Mexico 87545*

(Received 29 May 1992)

High-order scattering is found to be essential for the convergence of the multiple-scattering (MS) theory of x-ray-absorption fine structure, both in the near-edge and the extended regimes. These contributions are calculated using an *ab initio* curved-wave scattering-matrix formalism. Convergence to full MS accuracy is demonstrated for fcc Cu, as well as for molecular O₂ and N₂, where our approach provides a high-order MS interpretation of the σ^* shape resonances.

PACS numbers: 78.70.Dm, 71.10.+x, 79.60.-i

Curved-wave multiple-scattering (MS) theory [1] provides a unified theory for x-ray-absorption fine structure (XAFS) that encompasses both the extended (EXAFS) and near-edge (NEXAFS) regimes. When carried to all orders, this theory is equivalent to exact treatments based on wave functions and Hamiltonian diagonalizations. However, because present computational methods have limited applicability (such as to low-order MS [2], full MS at low energies only [3], or MS in small clusters [4]), there has been considerable speculation and controversy [1-4] about the nature and extent of MS in XAFS (e.g., on the need for full MS in NEXAFS or the importance of nonshadowing MS in EXAFS). In this Letter we introduce the first unified high-order MS treatment of XAFS with sufficient speed and accuracy to treat extended systems at both low and high energies. We find that neither full-MS nor low-order-MS theories are fully satisfactory; low-order theories generally contain too little MS, while much of that in full-MS theories is smeared out by inelastic losses and thermal disorder. We show this using high-order MS calculations for fcc Cu and for molecular O₂ and N₂. We find that the MS expansion for Cu with up to 7 scatterers and about 10⁵ paths converges to broadened band-structure results, while calculations with about 10² paths yield agreement with experiment out to 8.5 Å. Similarly, the MS expansion for O₂ and N₂ with up to 13 backscatterings converges to full MS $X\alpha$ -scattered-wave ($X\alpha$ -SW) calculations. Our approach also leads to a MS interpretation of the σ^* shape resonances [5] that are observed in NEXAFS and greatly simplifies their calculation. We demonstrate that such resonances are special XAFS peaks, whose asymmetry and location result from coherent high-order MS.

Our XAFS calculations are based on an automated implementation of (i) the curved-wave MS formalism of Rehr and Albers (RA) [6], (ii) an efficient method for enumerating MS paths, (iii) *ab initio* scattering potentials and phase shifts that include inelastic losses [7], and (iv) MS Debye-Waller factors. We calculate the normalized XAFS $\chi = (\mu - \mu_0)/\mu_0$, where μ is the x-ray-absorption coefficient and μ_0 the smooth atomiclike background.

The absorption μ is proportional to the projected photoelectron density of states or, equivalently, to the imaginary part of a Green's-function matrix element. More precisely, the MS expansion for the polarization-averaged K -shell XAFS is given by a sum over all scattering paths Γ , $\chi = \sum_{\Gamma} \text{Im} \langle e^{2i\delta_1} \sum_m \langle 1m | G t_N \cdots G t_2 G t_1 G | 1m \rangle \rangle$ (in matrix notation). Here G is a free-electron propagator, t_i is the scattering t matrix at site i , δ_1 is the $l = 1$ partial-wave phase shift at the absorbing atom, and the outer brackets indicate a thermal and configurational average. The efficiency of the RA approach is due to a separable representation of the electron propagators; it gives an accurate curved-wave XAFS formula analogous to that with the plane-wave approximation, but with scattering amplitudes $f(\theta)$ replaced by low-order (typically 6×6) matrices F . For an N -leg path Γ with scatterers at $\mathbf{R}_1, \mathbf{R}_2, \dots, \mathbf{R}_N = \mathbf{R}_0$ we obtain

$$\chi_{\Gamma}(p) = \text{Im} S_0^2 \frac{e^{i(\rho_1 + \rho_2 + \dots + \rho_N + 2\delta_1)}}{\rho_1 \rho_2 \cdots \rho_N} e^{-\sigma_T^2 p^2 / 2} \times \text{Tr} M F^N \cdots F^2 F^1. \quad (1)$$

Here $\rho_i = p(\mathbf{R}_i - \mathbf{R}_{i-1})$, $p = \sqrt{E - V_{\text{mt}}}$ is the photoelectron momentum measured with respect to the muffin-tin zero (in Rydberg atomic units), F^i is the scattering matrix at site i , M is the $l = 1$ termination matrix, S_0^2 is a many-body correction factor, and σ_T^2 is the mean-square variation in total path length R_t . The RA approach overcomes the computational bottleneck of the usual angular momentum basis $|lm\rangle$. For EXAFS, $l_{\text{max}} \cong 15-25$, which implies propagator-matrix dimensions of order 400-1000. Indeed, this bottleneck generally limits exact methods to the near-edge region or to triple scattering. We have verified the adequacy of 6×6 matrices by using z -axis propagators [6] that are virtually exact, but significantly slower computationally. We have also found that the approaches based on the plane-wave or small-atom approximations [1] have unacceptable errors for many paths. We illustrate our method with several examples.

Our first example is a comparison between our approach and broadened linear-augmented-plane-wave

(LAPW) band-structure calculations for Cu [8]. Because of its close-packed structure and strong scattering potentials Cu poses a severe test for MS theories. To avoid ambiguity we used the same self-consistent potentials, i.e., the same real phase shifts ($0 \leq l \leq 10$) [8], and essentially the same broadening. The band-structure results were broadened by a Lorentzian of width $\gamma = 8$ eV, while a constant imaginary potential $\text{Im}V = -\gamma/2 = -4$ eV was included in our propagators; these values give a good approximation to the observed mean free path. Making our approach practicable required the solution of another computational bottleneck, namely, the proliferation of paths. In fcc Cu there are of order 10^6 paths of length less than the typical mean free path of about 20 Å, which sets the minimum cluster size needed for full MS calculations. This number of paths is already impractically large, and we therefore used filters in our path enumeration scheme to reduce the number of paths being considered [9]. This was done with a constructive heap algorithm with cutoffs such that only paths of length less than some cutoff distance and amplitude larger than a given cutoff value are retained in the heap. Physically equivalent paths are sorted using an $N \log_2 N$ hash sort, and only those with amplitudes above a second cutoff are retained. For computational speed, plane-wave amplitudes are used for these estimates. With this parsing algorithm only a few percent of the paths need to be calculated. As a check on our path filters, the first 108 000 unique paths with length ≤ 18.4 Å were calculated with and without cutoff criteria, and showed no appreciable difference in the XAFS. A further study of convergence between 18.4 and 23.4 Å involved relaxing the criteria to double the number of paths considered, and again showed no appreciable change. The total cen-

tral processing unit time for the calculations was about 3 Cray Y/MP hours. Our results are summarized in Fig. 1, which compares the band-structure $l = 1$ projected density of states with our MS calculations. Note that our results are approximately converged at all energies. Also shown is an intermediate calculation with MS paths only out to 18.4 Å; note that the large peaks near 100, 140, and 160 eV cannot be duplicated with only these paths. These calculations show that high-order MS is essential to reproduce the full XAFS spectrum.

Our second example is a comparison of our approach with XAFS experiment for Cu at 190 K [10]. We focus in this example on XAFS in position space, i.e., on the minimum number of MS paths needed to treat XAFS contributions out to a given maximum path length. This approach is useful in the analysis of XAFS experiments, where long-path MS can be eliminated by Fourier filtering [11]. We used scattering phase shifts based on overlapped relativistic-atom muffin-tin potentials which take the core-hole potential and the self-energy into account; they were calculated using our *ab initio* XAFS cluster code [7], with an improved treatment of low-energy losses [12]. Though not self-consistent, these yield a good approximation to the scattering potential in Cu [7]. Our treatment explicitly includes MS Debye-Waller factors based on radial disorder, i.e., $\sigma_F^2 = \sum_{ij} \langle (\mathbf{u}_i - \mathbf{u}_{i'}) \cdot \hat{\mathbf{R}}_{ii'} (\mathbf{u}_j - \mathbf{u}_{j'}) \cdot \hat{\mathbf{R}}_{jj'} \rangle$, where $\mathbf{R}_{ij} = \mathbf{R}_i - \mathbf{R}_j$, $i' = i + 1$, $j' = j + 1$, and the displacement-displacement correlation functions are approximated using an isotropic Debye model [13] with Debye temperature $\Theta_D = 315$ K for Cu. Although better approximations for thermal disorder and inelastic losses would be desirable, our results for the XAFS Fourier transform $\tilde{\chi}(R_t/2)$ (Fig. 2) are in reasonable agreement with exper-

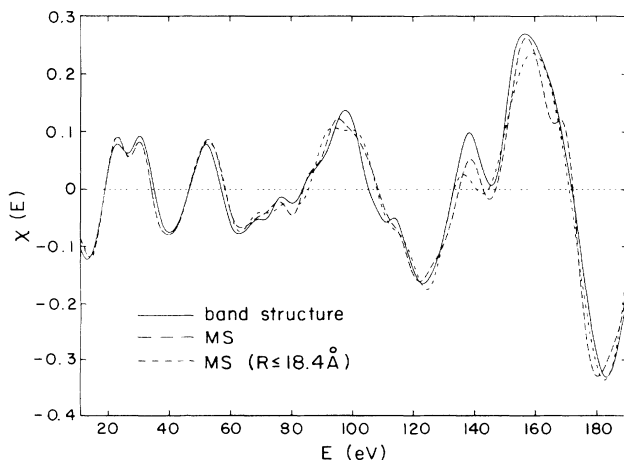


FIG. 1. Comparison of 8-eV Lorentzian broadened band-structure calculations of Cu XAFS (solid line) with high-order MS calculations of χ from this work: (long dashes) subset of MS paths with length $R_t \leq 23.4$ Å and single-scattering paths to 53.1 Å, and (short dashes) subset of SS and MS paths with $R_t \leq 18.4$ Å.

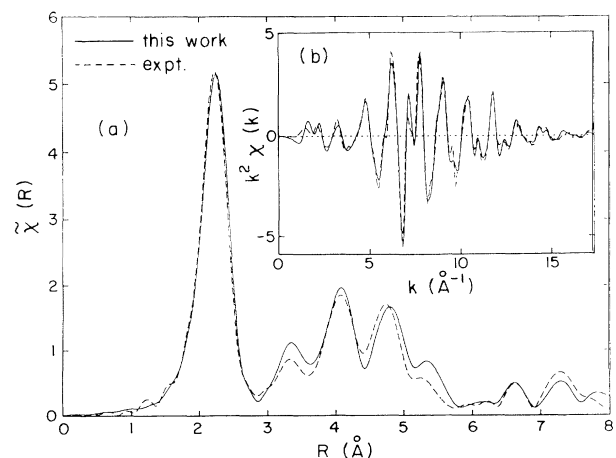


FIG. 2. Comparison of high-order MS calculations of Cu XAFS from this work with $S_0^2 = 0.906$ (solid line) and from XAFS experiment at 190 K (dashed line): (a) position space Fourier transform $\tilde{\chi}(R)$ and (b) in momentum space, $k^2 \chi(k)$. Here k is defined with respect to the Fermi energy, $k = \sqrt{E - E_F}$.

iment *with only one adjustable parameter*, an overall amplitude factor $S_0^2 = 0.906$ (the value of the Fermi energy was chosen to match the calculations). We find that just 15 of the 32 total paths with $R_t/2 \leq 5.1 \text{ \AA}$ survive cutoff filters set at 4% of the mean first-shell XAFS amplitude and suffice to describe $\chi(R)$ out to the fourth shell; none of these paths has more than triple scattering. Moreover, only 54 of the 17 134 unique paths with $R_t/2 \leq 8.466 \text{ \AA}$, with the same cutoff, suffice out to the twelfth shell and, of those 54, paths with 5 and 6 legs were found to be collinear.

For our next examples, we compare our MS calculations for molecular O_2 and N_2 with theory and experiment. Such calculations provide another severe test for MS theories because of the short bond length and strong low-energy scattering in low- Z atoms. A goal is to understand the σ^* shape resonances. These peaks are of much interest since their locations in energy are correlated with bond length [14]. The characteristic asymmetry of the peaks is similar to that of three-dimensional square-well resonances [15], but its fundamental origin was not, heretofore, understood. Recently it was shown that the σ^* resonances are well described by $X\alpha$ -SW calculations and correspond to the first enhanced XAFS oscillation [16], while Tyson *et al.* [4] have argued that the shape of a resonance is due to constructive interference of an infinite or large number of MS paths. We now give an alternative XAFS interpretation based on high-order MS. In particular we show that the resonances observed in O_2 and N_2 can be explained simply by the confluence of a finite number of MS contributions from repeated bounces between the two scattering sites. Our calculations were carried out with an "extended-continuum" (cf. Tyson *et al.* [4]) modification of our code, with the self-energy cor-

rection set to zero below the Fermi level, and again with molecular potentials and phase shifts from our cluster code [7]. The results for O_2 are shown in Fig. 3 for $p \geq 2.2 \text{ \AA}^{-1}$, below which the MS expansion fails to converge. Figure 3(a) shows how the resonance grows and sharpens as successive MS paths are added. The overall agreement with $X\alpha$ -SW calculations [16] is surprising in view of the simplicity of our scattering potential, and suggests that self-consistency and the outer-sphere potential are less important than the molecular potential within the molecule for scattering calculations. A closer analysis reveals that several factors, especially the strong backscattering amplitude and the coherence at resonance of the MS phases, govern the nature of the resonance. From Eq. (1) the MS phases vary as $(n+1)pR + 2\delta_1 + \Phi_n$, where R is the near-neighbor distance and n is the number of backscatterings. Thus the condition for constructive interference of successive MS paths is $2pR + 2\Delta\Phi = 2m\pi$ where $2\Delta\Phi = \Phi_{n+2} - \Phi_n$ and m is an integer, independent of δ_1 . Hence the peak location(s) satisfies

$$p = (m\pi - \Delta\Phi)/R, \quad (2)$$

which is a quantitative generalization of Natoli's rule [14]. In general, where more than a single bond length is involved, the location of shape-resonance peaks may be expected to correspond to a stationary phase point (modulo 2π) of some subset of MS paths. For diatomic molecules, $\Delta\Phi$ is approximately twice the backscattering phase. Our value for the peak location $p = 2.54$ is in reasonable agreement with the self-consistent $X\alpha$ -SW value $p = 2.7$ [16]. Figure 3(b) shows that the individual contributions χ_n from each MS path are restricted to successively lower wave numbers. This observation suggests a fundamental difference between NEXAFS and EXAFS on the basis of MS content. This is due in part to the MS Debye-Waller factors $\exp[-(n+1)^2\sigma^2 p^2/2]$, where for O_2 at 300 K, $\sigma^2 = 0.00136 \text{ \AA}^2$. These factors can dominate convergence of the MS expansion for large n , since the amplitudes vary only as $|F/\rho|^n$. However, in cases where $|F/\rho| > 1$, the number of terms required to achieve convergence may be so large that the path-by-path approach implemented here is impractical. Similar calculations for N_2 (cf. Fig. 4) indicate that the shape of the resonance is in good agreement with experiment [15]. In this comparison the experimental $\chi = (\mu - \mu_0)/\mu_0$ from polarized data is multiplied by a factor 1/3 to compare with our unpolarized calculation, and a factor $S_0^2 = 0.8$ was used in the theory.

In conclusion, we have developed a high-order MS approach that permits a unified treatment of XAFS at both low and high energies [17]. A more complete account of this work will be given elsewhere [18]. Our path-by-path approach has a number of advantages over exact "black-box" methods. In particular, the method permits a geometrical interpretation of XAFS, handles many thousands of paths in arbitrarily large systems, builds in inelastic losses and disorder, and is easier to compute than

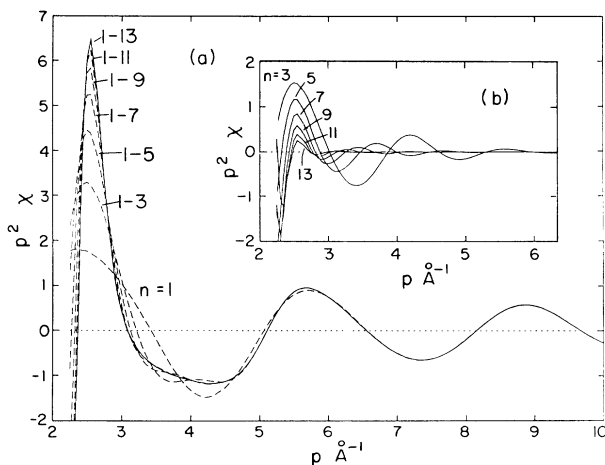


FIG. 3. MS calculations of the NEXAFS $p^2\chi$ vs photoelectron momentum p for molecular O_2 : (a) full spectrum with up to $n = 13$ backscattering (solid lines) and partial sums with all paths up to a given number of backscatterings (dashed lines); and (b) individual MS contributions $p^2\chi_n$ with n backscatterings. Here $p = \sqrt{E - V_{\text{mt}}}$.

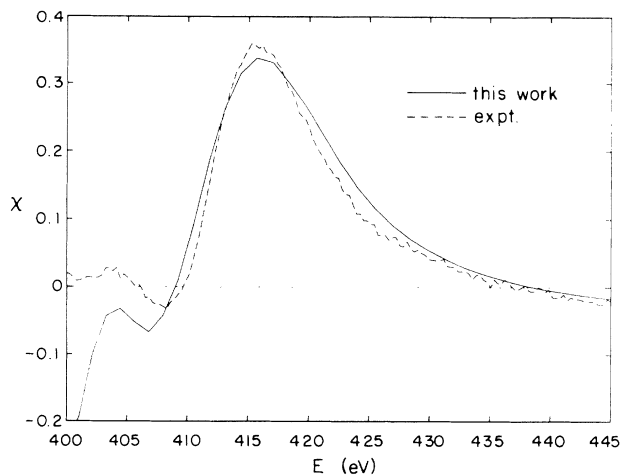


FIG. 4. Polarization-averaged MS calculations of χ for the σ^* resonance in N_2 plotted vs photoelectron energy E from this work with $S_0^2 = 0.8$ (solid line), and $\chi/3$ from polarized NEXAFS experiment [15] (dashed line); the factor of $1/3$ is a polarization correction.

wave-function methods. Our results support the observation that “shadowing” [1] is an important element of the MS in EXAFS, but also show that it is not the only consideration; noncollinear MS accounts for a substantial fraction of the total amplitude. We also find that a relatively small number of MS paths suffice to represent the contributions in XAFS from the first few shells, in support of position-space XAFS analysis methods [11]. Our results also confirm that noncollinear MS is important in the near edge [19], but they counter arguments that a full-MS treatment or full MS within a given shell is necessary [4]. Finally we have calculated MS Debye-Waller factors and shown that they can dominate convergence of the MS expansion.

We thank K. Baberschke, C. R. Natoli, and E. Stern for much helpful advice, D. Arvanitis, M. Newville, and B. Ravel for assistance with the experimental comparisons, and especially J. Stöhr for encouraging the shape resonance study and for informative discussions on NEXAFS. We also thank the Ohio Supercomputer Center for a grant of computer time. This work was supported in part by the U.S. Department of Energy (R.C.A.) and by DOE Grant No. DE-FG06-ER45415-A003 (J.J.R.).

[1] W. L. Schaich, Phys. Rev. B **8**, 4028 (1973); P. A. Lee

- and J. B. Pendry, Phys. Rev. B **11**, 2795 (1975); J. J. Barton and D. A. Shirley, Phys. Rev. B **32**, 1906 (1985); C. R. Natoli, M. Benfatto, and S. Doniach, Phys. Rev. A **34**, 4682 (1986).
- [2] J. E. Müller and W. L. Schaich, Phys. Rev. B **27**, 6489 (1983); J. J. Rehr, R. C. Albers, C. R. Natoli, and E. A. Stern, Phys. Rev. B **34**, 4350 (1986); S. J. Gurman, N. Binsted, and I. Ross, J. Phys. C **19**, 1845 (1986); M. F. Ruiz-Lopez, M. Loos, J. Goulon, M. Benfatto, and C. R. Natoli, Chem. Phys. **121**, 419 (1988); R. V. Vedrinski and L. A. Bugaev, J. Phys. B **24**, 1967 (1991).
- [3] J. E. Müller, O. Jepsen, and J. W. Wilkins, Solid State Commun. **42**, 365 (1982); E. E. Ellis and G. L. Goodman, Int. J. Quantum Chem. **25**, 185 (1984).
- [4] P. J. Durham, J. B. Pendry, and C. H. Hodges, Comput. Phys. Commun. **25**, 193 (1982); D. D. Vvedensky, D. K. Saldin, and J. B. Pendry, Comput. Phys. Commun. **40**, 421 (1986); T. A. Tyson, K. Hodgson, C. R. Natoli, and M. Benfatto, Stanford University report (to be published).
- [5] See, for example, *Principles, Applications, Techniques of EXAFS, SEXAFS, and XANES*, edited by D. C. Koningsberger and R. Prins (Wiley, New York, 1988); and J. Stöhr, *NEXAFS Spectroscopy* (Springer, Heidelberg, 1992).
- [6] J. J. Rehr and R. C. Albers, Phys. Rev. B **41**, 8139 (1990).
- [7] J. J. Rehr, J. Mustre de Leon, S. I. Zabinsky, and R. C. Albers, J. Am. Chem. Soc. **113**, 5135 (1991); J. Mustre de Leon, J. J. Rehr, S. I. Zabinsky, and R. C. Albers, Phys. Rev. B **44**, 4146 (1991).
- [8] R. C. Albers, A. K. McMahan, and J. E. Müller, Phys. Rev. B **31**, 3435 (1985).
- [9] S. I. Zabinsky and M. J. Eller (unpublished).
- [10] E. A. Stern, B. A. Bunker, and S. M. Heald, Phys. Rev. B **21**, 5521 (1980).
- [11] J. Mustre, Y. Yacoby, E. A. Stern, and J. J. Rehr, Phys. Rev. B **42**, 10843 (1990).
- [12] J. J. Quinn, Phys. Rev. **126**, 1453 (1962).
- [13] E. Sevilano, H. Meuth, and J. J. Rehr, Phys. Rev. B **20**, 4908 (1979); G. Beni and P. M. Platzman, Phys. Rev. B **14**, 9514 (1976).
- [14] C. R. Natoli, in *EXAFS and Near Edge Structure*, edited by A. Bianconi *et al.* (Springer, New York, 1983), p. 43.
- [15] D. Arvanitis, H. Rabus, L. Wenzel, and K. Baberschke, Z. Phys. D **11**, 219 (1989); Phys. Rev. B **40**, 6409 (1989).
- [16] J. Stöhr and K. R. Bauchspeiss, Phys. Rev. Lett. **67**, 3376 (1991).
- [17] Those interested in obtaining our MS code FEFF[©] should contact the authors.
- [18] R. C. Albers, S. I. Zabinsky, and J. J. Rehr (unpublished).
- [19] G. Bunker and E. A. Stern, Phys. Rev. Lett. **52**, 1940 (1984).